Integral boundary conditions for the time-dependent Schrödinger equation: Atom in a laser field

A. M. Ermolaev*
Physique Théorique, Faculté des Sciences, Université Libre de Bruxelles, Campus Plaine, PC 227, B-1050, Bruxelles, Belgium

I. V. Puzynin and A. V. Selin†
Laboratory of Computing Techniques and Automation, Joint Institute for Nuclear Research, 141980, Dubna, Russian Federation

S. I. Vinitsky
Bogoliubov Laboratory of Theoretical Physics, Joint Institute for Nuclear Research, 141980, Dubna, Russian Federation
(Received 7 June 1999)

We formulate exact integral boundary conditions for a solution of the time-dependent Schrödinger equation that describes an atom interacting, in the dipole approximation, with a laser pulse. These conditions are imposed on a surface (boundary) which is usually chosen at a finite (but sufficiently remote) distance from the atom where the motion of electrons can be assumed to be semiclassical. For the numerical integration of the Schrödinger equation, these boundary conditions may be used to replace mask functions and diffuse absorbing potentials applied at the edge of the integration grid. These latter are usually introduced in order to (approximately) compensate for unphysical reflection which occurs at the boundary of a finite region if a zero-value condition is imposed there on the solution. The present method allows one to reduce significantly the size of the space domain needed for numerical integration. Considering the numerical solution for a one-dimensional model, we demonstrate the effectiveness of our approach in comparison with some other numerical methods. [S1050-2947(99)10412-8]

PACS number(s): 42.50.Hz, 32.80.Wr, 32.80.Fb, 31.15.−p

I. INTRODUCTION

Several nonperturbative theories such as Floquet [1], Sturmian-Floquet [2], and *R*-matrix–Floquet [3] methods, have been developed to treat the time-dependent Schrödinger equation (TDSE) for an atom interacting with the classical laser field. These methods are particularly suited for moderate intensities and long laser pulses. However, experimental techniques are now moving towards generating superintense and supershort laser pulses. New computational methods are required to accommodate these extreme experimental conditions. The numerical solution of the TDSE on a time-space grid is a recognized powerful and universal method. The wave-packet dynamics of atom-laser interactions can be studied in great detail. This approach has been found particularly important for the adequate description of such processes as multiphoton ionization (MPI), stabilization, and high-harmonics generation. It has been extensively explored with one-dimensional models [4] as well as for real atomic systems. The TDSE calculations on atomic hydrogen [5], on atomic helium [6], on the Coulomb explosion of the H_2^+ molecule [7], as well as the time-dependent calculations on some one- and two-electron linear molecular ions [8] have been reported by several groups. The interrelation between the high-frequency Floquet (HFF) theory [9] and the TDSE method which deals with the wave-packet dynamics, has been recently analyzed in Ref. [10].

Despite the marked success of TDSE calculations and the development of several highly efficient numerical grid methods, including the lattice methods (see, e.g., Refs. [10,11]), certain practical limitations of the standard approach have now become apparent. They will be discussed below, within the method of integral boundary conditions (IBC) proposed in the present work.

The organization of the paper is as follows. In Sec. II, we give references to other numerical methods and we outline the main elements of the suggested IBC approach. In Sec. III, the derivation of the boundary conditions with the help of the integral equation for a Green's function is carried out for the general three-dimensional case. The cases of a spherical boundary and the Coulombic case are considered separately. In Sec. IV, we consider the one-dimensional (1D) case and formulate some relations needed for calculating the final spectral densities for the electron via the solution obtained in a finite region of space. In Sec. V, a numerical (Crank-Nicholson-Galerkin) method is formulated which uses a finite difference representation of the integral boundary conditions. In Sec. VI, we apply our IBC theory to the solution of a model-1D TDSE and discuss the results, in comparison with the complex coordinate contour (CC) and rigid boundary methods as well as with a method recently suggested by Boucke *et al.* [12]. Section VII concludes the paper.

Atomic units are used throughout the paper.

II. GENERAL REMARKS

For the laser-induced time evolution of the initial atomic state, the quantum-mechanical problem

$$i\partial_t \Psi(\mathbf{x},t) = H(t)\Psi(\mathbf{x},t) \tag{2.1}$$

is formulated as an initial value problem in an infinite do-

*Electronic address: ermolaev@ulb.ac.be
†Electronic address: selin@thsun1.jinr.ru

main of the configuration space $\mathbb{R}^3$ with the requirement that the wave function vanishes at infinity.

In the case of a one-electron atom which is presently considered, the Hamiltonian $H(t)$ in Eq. (2.1) is taken to be

$$H(t)=\frac{1}{2}\left(\mathbf{p}-\frac{e}{c}\mathbf{A}\right)^2+V(\mathbf{x}), \tag{2.2}$$

where $\mathbf{x}$ and $\mathbf{p}=-i\boldsymbol{\nabla}_{\mathbf{x}}$ are the position and momentum vectors of the electron, $V(\mathbf{x})$ is the atomic potential, and $\mathbf{A}$ is the vector potential of the classical electromagnetic field interacting with the atom; $c\approx 137$ is the velocity of light and e is the electron charge. In the dipole approximation which will be considered in this paper, $\mathbf{A}$ is a function of time t only. The electric field $\boldsymbol{\mathcal{E}}(t)$ due to $\mathbf{A}$ is given by $\boldsymbol{\mathcal{E}}(t)=-(1/c)\partial_t\mathbf{A}(t)$.

The numerical solution of Eq. (2.1), is usually carried out with the zero-value boundary condition imposed at a finite distance R_0 from the atom:

$$|\Psi(\mathbf{x},t)|=0, \quad |\mathbf{x}|=R_0, \quad \text{for all} \quad t. \tag{2.3}$$

Once the space domain is chosen to be finite, retaining some rigid boundary conditions causes unphysical reflection of the wave packet at the boundary and the reflected part of the packet is fed back into the system. Various techniques have been developed in order to compensate for the effect. The correction is achieved by either introducing an absorbing component into the atomic potential [13], or using mask functions [14]. An extension of the latter approach by splitting the wave function into two parts (for the interaction and asymptotic regions), introducing two complementary mask functions, and propagating two parts of the solution separately, has been considered in Ref. [15]. In the series of papers, the boundary correction has been considered by introducing complex coordinate contours [16]. However, by its nature, these corrections, generally speaking, have to be made at a large distance from the atom and they are approximate. Moreover, the domain of the configuration space where the solution has to be accurately obtained, may be large for ionization rate problems and even larger for treating MPI [17]. Therefore, though absorbing boundaries and mask functions work as a practical prescription, they do not relieve the numerical integration methods from the necessity of using overextended space grids.

A possible way of resolving these difficulties is to reformulate the problem and impose some conditions on an intermediate surface. For time-independent quantal problems, a variety of theoretical methods is known, such as, for example, the R-matrix method [18] and the finite-range method [19], where either a partial or full scattering problem is formulated within a finite domain of $\mathbb{R}^3$. We also note an extension of the R-matrix method to time-dependent problems [20]. The present work also uses a partition of the configuration space though in a context different from either one of the above methods.

In a recent paper, Boucke *et al.* [12] have suggested a particular way of imposing integral boundary conditions (IBC). They applied the IBC to a one-dimensional atom with a short-range potential in a strong laser field, within the electric-dipole approximation. Their results demonstrate a certain advantage of the method in calculating the above threshold ionization (ATI) and ionization rates. Their treatment, however, assumes the field-free asymptotic motion of the electron which is not a very accurate assumption, particularly for strong fields and long-range potentials. Also, as a consequence of their approach, it was necessary to carry out all calculations in the Kramers-Henneberger frame [21] where the interaction is localized.

In the present paper, we consider a more general IBC approach based on a theory of the parabolic potentials of the simple and double layers. We note that the reduction of the original differential equations to an integral form using the Green's functions, is a method which has been known in mathematical physics for a long time. Though it had been applied before to elliptic, hyperbolic, and parabolic equations [22], apparently, it has not been used yet for the time-dependent Schrödinger equation. In our formulation, we use the integral form of the equation to impose a constraint on the solution of the initial value problem. The choice of the surface where the constraint has to be applied should be made such that it would assure the correct (semiclassical) asymptotic behavior of the TDSE solution in the external region of the configuration space. The case of a short-range potential is considered at length. In principle, the proposed method is free from some restrictions imposed in Ref. [12]. Moreover, it can also be used for a general semiclassical construction of the asymptotic Green's functions [23,24]. As an example, a construction of the Green's function in the case of a Coulomb potential will be also considered.

III. BOUNDARY CONDITIONS

A. Parabolic potentials

We are considering the general case of a three-dimensional space $\mathbb{R}^3$. Let us denote via $G(\mathbf{x},t;\mathbf{x}',t')$ the time-dependent Green's function of the original TDSE (2.1). This function is the solution of the problem

$$L_{\mathbf{x},t}G(\mathbf{x},t;\mathbf{x}',t')=0, \quad t>t', \quad \mathbf{x},\mathbf{x}'\in\mathbb{R}^3, \tag{3.1}$$

where $L_{\mathbf{x},t}=i\partial_t-H(\mathbf{x},t)$, and the conjugate problem

$$L^*_{\mathbf{x}',t'}G(\mathbf{x},t;\mathbf{x}',t')=0, \quad t>t', \quad \mathbf{x},\mathbf{x}'\in\mathbb{R}^3, \tag{3.2}$$

where $L^*_{\mathbf{x}',t'}=-i\partial_{t'}-H^*(\mathbf{x}',t')$. The same initial condition

$$G(\mathbf{x},t;\mathbf{x}',t')\to\delta^{(3)}(\mathbf{x}-\mathbf{x}'), \quad t'\to t, t>t' \tag{3.3}$$

is applied in both cases. Here the operator H^* is complex conjugate of the Hermitian Hamiltonian H. Note that for arbitrary functions $u(\mathbf{x},t)$ and $v(\mathbf{x},t)$ the expression $u(\mathbf{x}',t')L_{\mathbf{x}',t'}v(\mathbf{x}',t')-v(\mathbf{x}',t')L^*_{\mathbf{x}',t'}u(\mathbf{x}',t')$ can be transformed into the divergence form

$$uL_{\mathbf{x}',t'}v-vL^*_{\mathbf{x}'t'}u = i\partial_{t'}(uv)+\frac{1}{2}\operatorname{div}_{\mathbf{x}'}(u\mathbf{D}_{\mathbf{x}',t'}v-v\mathbf{D}^*_{\mathbf{x}',t'}u), \tag{3.4}$$

where the differential operator $\mathbf{D}_{\mathbf{x},t}$ is given by

$$\mathbf{D}_{\mathbf{x},t} \equiv \boldsymbol{\nabla}_{\mathbf{x}} - i\frac{e}{c}\mathbf{A}(\mathbf{x},t). \tag{3.5}$$

Integrating Eq. (3.4) over a domain of the space $\mathbb{R}^3$ and time t gives the well-known Green's identity.

Let W be an arbitrary finite region of $\mathbb{R}^3$ which includes the atomic nucleus and is bounded by a piecewise smooth surface σ. The exterior to W will be denoted as usual via $\mathbb{R}^3 \setminus W$. Let us take in Eq. (3.4) the function $u(\mathbf{x}',t')$ to be the Green's function $G(\mathbf{x},t+\epsilon;\mathbf{x}',t')$, $\epsilon>0$, and the function $v(\mathbf{x}',t')$ to be the square-integrable solution $\Psi(\mathbf{x}',t')$ of the original TDSE,

$$L_{\mathbf{x},t}\Psi(\mathbf{x},t) = 0, \tag{3.6}$$

with specified initial conditions at $t=t_0$. We integrate the identity (3.4) with respect to coordinate $\mathbf{x}'$ over the domain $\mathbb{R}^3 \setminus W$ and with respect to time t' from t_0 to t. The left-hand side of Eq. (3.4) is identically zero due to Eqs. (3.2) and (3.6), and the right-hand side can be integrated by parts. After taking the limit $\epsilon \to 0$, one finds

$$0 = i\Psi(\mathbf{x},t)\chi_W(\mathbf{x}) - i\int_{\mathbb{R}^3\setminus W} d^3\mathbf{x}'\, G(\mathbf{x},t;\mathbf{x}',t_0)\Psi(\mathbf{x}',t_0) - \frac{1}{2}\int_{t_0}^{t} dt' \int_{\sigma} d\boldsymbol{\sigma}' \cdot \{G\mathbf{D}'\Psi(\mathbf{x}'_\sigma,t') - \Psi(\mathbf{x}'_\sigma,t')\mathbf{D}^{*\prime}G\}, \tag{3.7}$$

where $d\boldsymbol{\sigma}$ is a vector element of the surface σ which is pointed outward W. Here it has been used that the wave function at large distances tends to zero sufficiently fast so that the surface integral taken over the outer surface at infinity vanishes.

The function χ_W in Eq. (3.7) is a characteristic function discontinuous in $\mathbb{R}^3$, which is defined [25] as follows:[1]

$$\chi_W(\mathbf{x}) \equiv \lim_{\epsilon\to 0}\int_{\mathbb{R}^3\setminus W} d^3\mathbf{x}'\, G(\mathbf{x}',t+\epsilon,\mathbf{x}',t) = \begin{cases} 1, & \mathbf{x}\in\mathbb{R}^3\setminus W, \mathbf{x}\notin\sigma, \\ \frac{1}{2}, & \mathbf{x}\in\sigma, \\ 0, & \mathbf{x}\in W, \mathbf{x}\notin\sigma. \end{cases} \tag{3.8}$$

Let us denote by μ and ν the values of the wave function and its normal derivative on σ, thus

$$\Psi|_\sigma = \mu(\mathbf{x}_\sigma,t), \quad \mathbf{n}_\sigma\cdot\mathbf{D}_{x,t}\Psi|_\sigma = \nu(\mathbf{x}_\sigma,t), \tag{3.9}$$

where $\mathbf{n}_\sigma$ is a unit vector normal to the surface σ and directed outward W. We introduce functions v, w, and F associated with these quantities, according to

$$v(\mathbf{x},t) = -\int_{t_0}^{t} dt' \int_{\sigma} d\sigma'\, \nu(\mathbf{x}'_\sigma,t')G(\mathbf{x},t,\mathbf{x}'_\sigma,t'), \tag{3.10}$$

$$w(\mathbf{x},t) = \int_{t_0}^{t} dt' \int_{\sigma} d\sigma'\, \mu(\mathbf{x}'_\sigma,t')\, \mathbf{n}'_\sigma\cdot\mathbf{D}^*_{x',t'}G(\mathbf{x},t,\mathbf{x}'_\sigma,t'), \tag{3.11}$$

$$F(\mathbf{x},t) = \int_{\mathbb{R}^3\setminus W} d^3\mathbf{x}'\, \Psi(\mathbf{x}',t_0)G(\mathbf{x},t,\mathbf{x}',t_0). \tag{3.12}$$

where t_0 is the initial moment of time for the initial-value problem (2.1).

Due to the singularity of G, the quantities defined by Eqs. (3.10)–(3.12) can be given a classical interpretation as potentials generated by some surface and volume mass distributions. Similar potentials appear in the general theory of parabolic equations [25]. In the present case of the Schrödinger equation, we shall use the same terminology as in Ref. [25] and refer to Eqs. (3.10)–(3.12) as parabolic potentials. Then v is a simple-layer parabolic potential with the surface density ν, w is a double-layer parabolic potential with the surface density μ, and F is the initial-value parabolic potential. Making use of these quantities, Eq. (3.7) can be rewritten as follows:

$$\Psi(\mathbf{x},t)\chi_W = F(\mathbf{x},t) + \frac{i}{2}\{v(\mathbf{x},t)+w(\mathbf{x},t)\}, \quad \mathbf{x}\in\mathbb{R}^3, \tag{3.13}$$

for any $t>t_0$. This formula is a general relation satisfied by the solution of Eq. (2.1) for an arbitrary choice of the region W enclosed by a surface σ. It has a form of an integral equation which determines the wave function $\Psi(\mathbf{x},t)$ through the parabolic potentials (3.10)–(3.12). As these potentials are defined in terms of the full Green's function, Eq. (3.13) can be used for constructing the solution of Eq. (2.1) only within some method of successive approximations.

B. Integral boundary conditions

Now we shall discuss an application of Eq. (3.13) which is important in the numerical solution of Eq. (2.1). Let us consider the special case where the point $\mathbf{x}$ is on the surface σ. Then Eq. (3.13) takes the form

$$\mu(\mathbf{x}_\sigma,t) = 2F(\mathbf{x}_\sigma,t) + i\{v(\mathbf{x}_\sigma,t)+w(\mathbf{x}_\sigma,t)\}. \tag{3.14}$$

This relation expresses the fact that values of the wave function μ and its normal derivatives ν on the surface σ cannot be arbitrary functions but must satisfy an integral constraint [26].

Equation (3.14) can also be obtained by considering the limiting passage in Eq. (3.13) as $\mathbf{x}\to\mathbf{x}_\sigma$, $\mathbf{x}\notin\sigma$. Then the continuity of the simple-layer potential and the discontinuity of the double-layer potential in the limit should be taken into account. For the potential w we have

$$\lim_{\mathbf{x}\to\mathbf{x}_\sigma} w(\mathbf{x},t) = \mp i\mu(\mathbf{x}_\sigma,t) + w(\mathbf{x}_\sigma,t), \tag{3.15}$$

[1]The convergence of the integral is assured by endowing the time variable t with an infinitesimal imaginary part which has the proper sign, $t\to te^{-i0}$.

where the upper sign $(-)$ corresponds to approaching the surface from outside and the lower sign $(+)$ corresponds to approaching it from inside the internal region W. Due to the continuity of the wave function, the limits of Eq. (3.13) from inside and outside of the surface σ give, of course, the same result as Eq. (3.14).

Equation (3.14) will be the starting point for the derivation of integral boundary conditions to be imposed on σ for the solution of TDSE (2.1) in internal domain W.

First, we shall consider the case of a fast-decaying atomic potential V such as, for instance, the short-range Yukawa potential. Let us denote via H_{as} the Hamiltonian H, Eq. (2.2), without the potential term V, i.e.,

$$H(t)=H_{as}(t)+V, \tag{3.16}$$

and consider the auxiliary problem

$$i\partial_t\tilde{\Psi}(\mathbf{x},t)=H_{as}(t)\tilde{\Psi}(\mathbf{x},t). \tag{3.17}$$

The corresponding Green's function of this problem will be denoted as $G_{as}(\mathbf{x},t;\mathbf{x}',t')$. Due to the fast decay of the potential V at $|\mathbf{x}|\to\infty$, an arbitrary solution of Eq. (2.1) satisfies also Eq. (3.17) in the asymptotic region.

It follows from Eq. (3.16), that

$$\begin{aligned}G(\mathbf{x},t,\mathbf{x}',t')&=G_{as}(\mathbf{x},t,\mathbf{x}',t')\\&\quad-i\int_{t'}^{t}dt''\int d^3\mathbf{x}''\,G_{as}(\mathbf{x},t,\mathbf{x}'',t'')\\&\quad\times V(\mathbf{x}'',t'')G(\mathbf{x}'',t'',\mathbf{x}',t'),\end{aligned} \tag{3.18}$$

where integration over $\mathbf{x}''$ extended to all configuration space $\mathbb{R}^3$.

We note that the problem (3.17) is simpler than the original Eq. (2.1) and, in some cases, Eq. (3.17) may have an analytical solution.

Due to the dipole approximation, the asymptotic Hamiltonian H_{as} is given in the velocity gauge by

$$H_{as}(t)=-\frac{1}{2}\Delta_{\mathbf{x}}+i\frac{e}{c}\mathbf{A}(t)\cdot\boldsymbol{\nabla}_{\mathbf{x}}, \tag{3.19}$$

where the term quadratic in $\mathbf{A}(t)$ has been removed from Eq. (2.1) by a simple phase transformation of the wave function Ψ.

The explicit form of the Green's function G_{as} of the TDSE with the Hamiltonian (3.19) is

$$G_{as}(\mathbf{x},t;\mathbf{x}',t')=\frac{e^{iS(\mathbf{x},t;\mathbf{x}',t')}}{[2\pi i(t-t')]^{3/2}},\quad t>t', \tag{3.20}$$

where S is the classical action for a particle in the field $\mathbf{A}(t)$ taken to be a function of the initial and the final position and time (the Hamilton principle function), that is,

$$S(\mathbf{x},t;\mathbf{x}',t')=\frac{[\mathbf{x}-\boldsymbol{\xi}(t)-\mathbf{x}'+\boldsymbol{\xi}(t')]^2}{2(t-t')} \tag{3.21}$$

and $\boldsymbol{\xi}(t)$ is the classical displacement of the electron due to the field given by

$$\boldsymbol{\xi}(t)=-\frac{e}{c}\int^{t}\mathbf{A}(\tau)d\tau. \tag{3.22}$$

The form (3.20) of the G_{as} is determined by the WKB approximation which gives the exact result for the TDSE with the Hamiltonian (3.19) [27]. This Green's function can also be obtained in a straightforward manner from an expansion in terms of the corresponding Volkov states $\Theta_{\mathbf{k}}(\mathbf{x},t)$,

$$\Theta_{\mathbf{k}}(\mathbf{x},t)=\exp\left\{i\mathbf{k}\cdot[\mathbf{x}-\boldsymbol{\xi}(t)]-\frac{i}{2}\mathbf{k}^2t\right\}. \tag{3.23}$$

Then

$$G_{as}(\mathbf{x},t,\mathbf{x}',t')=\int\frac{d^3\mathbf{k}}{(2\pi)^3}\Theta_{\mathbf{k}}(\mathbf{x},t)\Theta_{\mathbf{k}}^{*}(\mathbf{x}',t'). \tag{3.24}$$

Now we shall use the integral equation (3.18) to replace the full Green's function G in Eq. (3.14) by the asymptotic Green's function G_{as} as derived above, and obtain the asymptotic parabolic potentials.

Multiplying both sides of Eq. (3.18) by the density $\nu(\mathbf{x}',t')$ and integrating with respect to time t' from t_0 up to t and keeping the surface σ fixed, one finds that the simple-layer potential v satisfies the integral equation

$$\begin{aligned}v(\mathbf{x},t)&=v_{as}(\mathbf{x},t)-i\int_{t_0}^{t}dt''\int d^3\mathbf{x}''\,G_{as}(\mathbf{x},t,\mathbf{x}'',t'')\\&\quad\times V(\mathbf{x}'',t'')v(\mathbf{x}'',t'').\end{aligned} \tag{3.25}$$

Here the zero-order term v_{as} is a simple-layer parabolic potential constructed as in Eq. (3.10) but with the help of the asymptotic Green's function G_{as},

$$v_{as}(\mathbf{x},t)=-\int_{t_0}^{t}dt'\int_{\sigma}d\sigma'\,\nu(\mathbf{x}'_{\sigma},t')G_{as}(\mathbf{x},t,\mathbf{x}'_{\sigma},t'). \tag{3.26}$$

Similar integral equations can be obtained for the double-layer parabolic potentials w and w_{as} as well as for the initial-value parabolic potentials F and F_{as}.

The following form of the integral relation (3.13) is obtained by substituting in it the asymptotic equations derived above:

$$\begin{aligned}\Psi(\mathbf{x},t)\chi_W(\mathbf{x})&=F_{as}(\mathbf{x},t)+\frac{i}{2}\{v_{as}(\mathbf{x},t)+w_{as}(\mathbf{x},t)\}\\&\quad-i\int_{t_0}^{t}dt''\int d^3\mathbf{x}''\,G_{as}(\mathbf{x},t,\mathbf{x}'',t'')\\&\quad\times V(\mathbf{x}'',t'')\Psi(\mathbf{x}'',t'')\chi_W(\mathbf{x}'').\end{aligned} \tag{3.27}$$

The use of asymptotic parabolic potentials in Eq. (3.27) generally assures the correct asymptotic behavior of the wave function of the original problem (2.1).

If the potential $V(\mathbf{x},t)$ is a short-range potential, and the domain W contains the main region of action for V, then the last term in Eq. (3.27) is negligibly small since due to the presence of the characteristic function χ_W, the integration extends only outside W. Thus, in this case, the equation on

the boundary has the form (3.14) where the parabolic potentials are simply replaced by the asymptotic potentials, i.e.,

$$\mu(\mathbf{x}_\sigma,t)=2F_{as}(\mathbf{x}_\sigma,t)+i\{v_{as}(\mathbf{x}_\sigma,t)+w_{as}(\mathbf{x}_\sigma,t)\}. \tag{3.28}$$

This boundary condition is, generally, a linear, nonlocal relationship between the boundary and the initial value of the wave function. We also note that, for the potentials decaying too slowly, Eq. (3.27) may require the next iteration with respect to Ψ or some other methods of solution.

C. Spherical boundary of domain W

Now we consider a particular case where the surface σ of the domain W is a sphere σ_R of large radius $R \gg a_0$ where a_0 is an effective radius of interaction. For the sake of simplicity we assume also that the initial wave function $\Psi(\mathbf{x},t_0)$ is negligibly small in the outer domain beyond σ_R. Then the term $F_{as}(\mathbf{x},t)$ in Eq. (3.28) can be dropped. Thus, our task is to find the asymptotic expressions for the parabolic potentials v_{as} and w_{as} on the sphere σ_R. Let us denote $\hat{\mathbf{n}}=R^{-1}\mathbf{x}_\sigma$,

$$Q(t,t')=|R\hat{\mathbf{n}}-\boldsymbol{\xi}(t)+\boldsymbol{\xi}(t')|, \tag{3.29}$$

and

$$\hat{\boldsymbol{\omega}}(t,t')=\frac{R\hat{\mathbf{n}}-\boldsymbol{\xi}(t)+\boldsymbol{\xi}(t')}{|R\hat{\mathbf{n}}-\boldsymbol{\xi}(t)+\boldsymbol{\xi}(t')|}. \tag{3.30}$$

Making use of these notations, the Green's function (3.20) can be written as

$$G_{as}(R\hat{\mathbf{n}},t;R\hat{\mathbf{n}}',t')=\frac{\exp\left[i\dfrac{R^2+Q^2}{2(t-t')}\right]}{[2\pi i(t-t')]^{3/2}}\exp\left[-i\frac{RQ}{t-t'}\hat{\mathbf{n}}'\cdot\hat{\boldsymbol{\omega}}\right]. \tag{3.31}$$

The angle integration in Eq. (3.26) with the Green's function (3.31) over σ_R can be carried out by taking into account the leading contribution from the points of the stationary phase in the directions $\hat{\mathbf{n}}'=\pm\hat{\boldsymbol{\omega}}$. Indeed, the angular part of Eq. (3.31) has, as a distribution, the asymptotic representation

$$e^{-i\lambda\hat{\mathbf{n}}\cdot\hat{\boldsymbol{\omega}}}=\frac{2\pi i}{\lambda}\{e^{-i\lambda}\delta(\hat{\mathbf{n}},\hat{\boldsymbol{\omega}})-e^{i\lambda}\delta(\hat{\mathbf{n}},-\hat{\boldsymbol{\omega}})\}+O(\lambda^{-2}), \tag{3.32}$$

where $\delta(\hat{\mathbf{n}},\hat{\boldsymbol{\omega}})$ is the δ function on the unit sphere and $\lambda=(RQ/t-t')$. Thus, the angle integration in Eq. (3.26) yields for the potential v_{as}

$$v_{as}(R\hat{\mathbf{n}},t)\simeq-\int_{t_0}^{t}\frac{R}{Q}\frac{dt'}{\sqrt{2\pi i(t-t')}}\left\{\exp\left[i\frac{(Q-R)^2}{2(t-t')}\right]\nu(\hat{\boldsymbol{\omega}},t')-\exp\left[i\frac{(Q+R)^2}{2(t-t')}\right]\nu(-\hat{\boldsymbol{\omega}},t')\right\}. \tag{3.33}$$

Here we restrict our attention to such electric fields that the classical displacement (3.22) $\boldsymbol{\xi}(t)$ is bounded for all times. It means that the function $Q(t,t')$ in the last expression takes values close to R but it is never zero, provided that R is sufficiently large. Then the second term in the integral (3.33) can be neglected because it contains a rapidly oscillating exponential at $t'\to t$. To estimate the neglected quantity, let us consider the leading term of the asymptotic expansion of the following integral:

$$I(\lambda)=\int_{t_0}^{t}dt'(t-t')^{-\alpha}e^{i\lambda(t-t')^{-1}}g(t'),\quad \alpha<2, \tag{3.34}$$

where $\lambda\to+\infty$, and $g(t')$ is a smooth nonsingular function in the segment $[t_0,t]$. By changing variables, $\rho=(t-t')^{-1}$, this integral transforms to

$$I(\lambda)=\int_{(t-t_0)^{-1}}^{+\infty}\rho^{\alpha-2}\,d\rho\,e^{i\lambda\rho}g(t-\rho^{-1}). \tag{3.35}$$

Integrating by parts gives the leading asymptotic term, thus

$$I(\lambda)=-\frac{(t-t_0)^{2-\alpha}}{i\lambda}e^{i\lambda(t-t_0)^{-1}}g(t_0)+O(\lambda^{-2}). \tag{3.36}$$

Taking $\alpha=1/2$ and $\lambda=2R^2$ in Eq. (3.36), one finds that the absolute value of the estimated term in Eq. (3.33) is of order

$$\frac{(t-t_0)^{3/2}}{RQ(t,t_0)}|\nu(-\hat{\boldsymbol{\omega}}(t,t_0),t_0)|. \tag{3.37}$$

Here it should be taken into account that the values of μ and ν at the initial moment t_0 are negligibly small, hence the second term in Eq. (3.33) can be neglected.

The case of the potential w_{as} can be dealt with in a completely analogous manner. As a result, the asymptotic form of relation (3.28) is found to be as follows:

$$\mu(\hat{\mathbf{n}},t)=\int_{t_0}^{t}\frac{R}{Q}\frac{\exp\left[i\dfrac{(Q-R)^2}{2(t-t')}\right]dt'}{\sqrt{2\pi i(t-t')}}\times\left\{\mu(\hat{\boldsymbol{\omega}},t')\left(\frac{Q-R}{t-t'}-\frac{e}{c}\hat{\boldsymbol{\omega}}\cdot\mathbf{A}(t')\right)-i\nu(\hat{\boldsymbol{\omega}},t')\right\}. \tag{3.38}$$

In the particular case of $\mathbf{A}\equiv0$, this relation reduces to one obtained in Ref. [12].

D. Coulomb potential

Now we shall consider the case of a Coulomb potential. Due to a slow rate of decay, it causes the specific phase distortion in the time-independent Coulomb Green's function at large distances, in comparison with the short-range potentials. This effect should be taken into account while deriving the boundary conditions. Following the general method outlined above, we have to construct a semiclassical G_{as} which will be used in the exterior domain $\mathbb{R}^3\setminus W$. We shall achieve

that by considering an approximation $G_c(\mathbf{x},t;\mathbf{x}',t')$ to the time-dependent Coulomb Green's function which satisfies the following equation:

$$i\partial_t G_c = -\frac{1}{2}\Delta_{\mathbf{x}} G_c + i\frac{e}{c}\mathbf{A}\cdot\boldsymbol{\nabla}_{\mathbf{x}} G_c + \frac{\alpha}{|\mathbf{x}|}G_c, \qquad (3.39)$$

together with the initial condition (3.3). As follows from the physical arguments (see, e.g., Ref. [29]), the motion of the particle is semiclassical at distances much larger than Bohr radius. Thus, for our purposes, it should be possible to apply the WKB techniques [24]. The function G_c is sought as a product:

$$G_c = C(\mathbf{x},t;\mathbf{x}',t')e^{iS(\mathbf{x},t;\mathbf{x}',t')}, \qquad (3.40)$$

where C and S are arbitrary real-valued functions. Substituting Eq. (3.40) into Eq. (3.39) yields the following system:

$$\begin{cases} \partial_t C^2 + \mathrm{div}_{\mathbf{x}}\left\{ C^2\left(\boldsymbol{\nabla}_{\mathbf{x}} S - \frac{e}{c}\mathbf{A}\right)\right\} = 0, \\ \partial_t S + \frac{1}{2}(\boldsymbol{\nabla}_{\mathbf{x}} S)^2 - \frac{e}{c}\mathbf{A}\cdot\boldsymbol{\nabla}_{\mathbf{x}} S + \frac{\alpha}{|\mathbf{x}|} = \frac{\Delta_{\mathbf{x}} C}{C}. \end{cases} \qquad (3.41)$$

The first line in Eq. (3.41) is the continuity equation for the density C. The second line, with the right-hand side set to be zero, is the Hamilton-Jacobi equation for the action describing the classical motion of the atomic electron. The left-hand side of this equation is identically zero if the function S is taken to be the integral of the Lagrange function calculated along the classical trajectory of particle $\mathbf{X}(\tau;\mathbf{x},\mathbf{x}')$, with the end points $\mathbf{x}$ and $\mathbf{x}'$ for $\tau=t'$ and $\tau=t$, respectively. That is

$$S = \int_{t'}^{t} d\tau \left\{ \frac{\left[\dot{\mathbf{X}}(\tau) + \frac{e}{c}\mathbf{A}(\tau)\right]^2}{2} - \frac{\alpha}{|\mathbf{X}(\tau)|}\right\}. \qquad (3.42)$$

We note that if the Coulomb potential is absent in Eq. (3.41) then the exact trajectory $\mathbf{X}_0(\tau)$ is

$$\mathbf{X}_0(\tau) = \frac{\mathbf{x} - \boldsymbol{\xi}(t) - \mathbf{x}' + \boldsymbol{\xi}(t')}{t-t'}(\tau - t') + \boldsymbol{\xi}(\tau) - \boldsymbol{\xi}(t') + \mathbf{x}', \qquad (3.43)$$

and the action of Eq. (3.42) evaluated along this trajectory is exactly the expression (3.21). Moreover, if the density function C is taken to be independent of the space variables,

$$C = [2\pi i(t-t')]^{-3/2} \qquad (3.44)$$

then both equations in Eq. (3.41) are identically satisfied provided that $\alpha=0$. The resulting function coincides with the Green's function (3.20).

In the case of $\alpha\neq 0$, we shall introduce an approximation which is similar to the eikonal approximation for the time-independent case (see Ref. [28]). Namely, the solution of Eq. (3.41) is obtained by evaluating the action S in Eq. (3.42) along the free trajectory $\mathbf{X}_0(\tau)$ given by Eq. (3.43), i.e.,

$$S \approx S_0 - Z, \qquad (3.45)$$

where S_0 is the expression (3.21). In Eq. (3.45), the phase distortion Z is defined as

$$Z(\mathbf{x},t;\mathbf{x}',t') = \alpha\int_{t'}^{t}\frac{d\tau}{|\mathbf{X}_0(\tau)|}, \qquad (3.46)$$

and the density C is the same as above in Eq. (3.44). Note that this approximation does not work if the classical trajectory $\mathbf{X}_0(\tau)$ passes through the Coulomb center because in the latter case the integral (3.46) is not defined. Below we exclude this case from consideration.

In order to estimate an error in such a model, we first note that the function Z satisfies (within the assumptions stated above) the Laplace equation

$$\Delta_{\mathbf{x}} Z = 0. \qquad (3.47)$$

Thus, the continuity equation (3.41) holds exactly. Second, the action S, Eq. (3.45), satisfies the Hamilton-Jacobi equation in Eq. (3.41) only approximately. After some manipulations one finds that the error [thus, it is a relative error for the solution of Eq. (3.39) in the form of Eq. (3.40)] is

$$\frac{1}{2}(\boldsymbol{\nabla}_{\mathbf{x}} Z)^2 \sim \alpha^2\frac{(t-t')^2}{\rho^4}, \qquad (3.48)$$

where ρ is the distance of closest approach, from the Coulomb center to the trajectory $\mathbf{X}_0(\tau;\mathbf{x},\mathbf{x}')$. This estimate can be useful for choosing the grid size for the numerical integration of the TDSE if one uses the approximation to G_c considered above.

The phase distortion Z depends on the particular form of the electric field $\mathbf{A}(t)$ and it should be considered in each case separately. However, in the field-free case it is evaluated explicitly to give

$$Z^{(0)}(\mathbf{x},t;\mathbf{x}',t') = \alpha\frac{t-t'}{|\mathbf{x}-\mathbf{x}'|}\ln\frac{|\mathbf{x}||\mathbf{x}-\mathbf{x}'| + \mathbf{x}\cdot(\mathbf{x}-\mathbf{x}')}{|\mathbf{x}'||\mathbf{x}-\mathbf{x}'| + \mathbf{x}'\cdot(\mathbf{x}-\mathbf{x}')}. \qquad (3.49)$$

We note the formal correspondence between this expression and the asymptotic distortion term in the phase of the stationary Coulomb Green's function $G_c(\mathbf{x},\mathbf{x}',E+i0)$ [28] provided that one treats the factor $t-t'/|\mathbf{x}-\mathbf{x}'|$ in Eq. (3.49) as $(2E)^{-1/2}$.

Considering the field-free case for the spherical boundary of radius $R\gg 1$, in exactly the same way as it was done in Sec. III C, one finds the asymptotic form of the boundary equation (3.28) with the Coulomb corrections, as follows:

$$\mu(\hat{\mathbf{n}},t) = \int_{t_0}^{t}\frac{\exp\left[-i\frac{\alpha}{R}(t-t')\right]dt'}{\sqrt{2\pi i(t-t')}} \times\left\{-\frac{\alpha(t-t')}{2R^2}\mu(\hat{\mathbf{n}},t') - i\nu(\hat{\mathbf{n}},t')\right\}. \qquad (3.50)$$

Here we note that the knowledge of the asymptotic form of G_c in the singular direction $\hat{\mathbf{n}}'=-\hat{\mathbf{n}}$ is not required in the approximation (3.50).

IV. APPLICATION TO 1D PROBLEM

A. Boundary conditions

We assume that the potential $V(x)$ of a model 1D atom operates in the domain $W \in \mathbb{R}$ which is a finite interval $a_- < x < a_+$. Adjacent to it are two half-open intervals: $x < a_-$ (region I) and $x > a_+$ (region II) separated from W by the boundaries $x = a_\pm$. Let us denote the values of the wave function $\Psi(x,t)$ and its derivative $D_{x,t}\Psi(x,t) \equiv [\partial_x - ie/cA(t)]\Psi(x,t)$ at the boundaries of regions I and II as

$$\Psi(a_\mp,t) = \mu^{I,II}(t), \quad D_{x,t}\Psi(a_\mp,t) = \nu^{I,II}(t). \tag{4.1}$$

The Green's function G_{as} in the 1D case is

$$G_{as}(x,t;x',t') = \frac{e^{iS(x,t;x',t')}}{\sqrt{2\pi i(t-t')}}, \quad t > t', \tag{4.2}$$

where the action S is given by Eq. (3.21). The boundary equations (3.28) are then written as follows:

$$\mu^{I,II}(t) = 2F^{I,II}_{as}(a_\mp,t) + i\{\nu^{I,II}_{as}(a_\mp,t) + w^{I,II}_{as}(a_\mp,t)\}, \tag{4.3}$$

where the parabolic potentials are defined by

$$\nu^{I,II}_{as}(x,t) = \pm \int_{t_0}^{t} \frac{\nu^{I,II}(t')dt'}{\sqrt{2\pi i(t-t')}} e^{iS(x,t;a_\mp,t')}, \tag{4.4}$$

$$w^{I,II}_{as}(x,t) = \mp i \int_{t_0}^{t} \frac{\mu^{I,II}(t')dt'}{\sqrt{2\pi i(t-t')}} \times \left(\frac{\partial S}{\partial x'} + \frac{e}{c}A(t') \right) e^{iS(x,t;a_\mp,t')}, \tag{4.5}$$

$$F^{I,II}_{as}(x,t) = \int_{I,II} \frac{\Psi(x',t_0)dx'}{\sqrt{2\pi i(t-t_0)}} e^{iS(x,t;x',t_0)}. \tag{4.6}$$

Before proceeding farther, it is instructive to consider a special case where $V(x)$ is a zero-range potential determined by the boundary condition at the origin

$$\nu^{II}(0,t) - \nu^{I}(0,t) = 2\varkappa\mu(0,t). \tag{4.7}$$

This condition corresponds to the potential V of the form $\varkappa\delta(x)$. In this case, the domain W consists of one point, $x = 0$, that is $W = \{0\}$. It is easy to check that the half sum of Eqs. (4.3) gives, due to Eq. (4.7), a Volterra equation for $\Psi(0,t)$, thus

$$\Psi(0,t) = \int_{-\infty}^{+\infty} dx'\, G_{as}(0,t,x',t_0)\Psi(x',t_0) - i\varkappa \int_{t_0}^{t} dt' G_{as}(0,t,0,t')\Psi(0,t'). \tag{4.8}$$

This equation provides the complete solution $\Psi(x,t)$. Alternatively, it can be obtained directly from the original TDSE (for details see Ref. [30]).

This limiting case is a good illustration of our general conclusion: In the IBC method, the size of the region W where the numerical solution is to be found, depends only on the decaying properties of the potential V. As will be shown in the numerical example below, the suggested method of imposing boundary conditions allows the region W to be chosen sufficiently small, despite the presence of a strong laser electric field.

B. Evaluation of spectrum

We shall now consider how the energy spectrum of photoelectrons can be extracted using solution (2.1) which is known in the internal domain W. It will be assumed that the pulse of the electric field has a finite duration and the corresponding vector potential $A(t)$ is equal to zero before and after the action of the pulse. Let the electron be initially in a bound state

$$\Psi_n(x,t) = e^{-iE_n t}\psi_n(x). \tag{4.9}$$

The transition amplitude $\mathcal{A}_{qn}$ to the final continuum states

$$\Psi^{(-)}_{1,2E} = e^{-iEt}\psi^{(-)}_{1,2E} \tag{4.10}$$

is given by the usual rule

$$\mathcal{A}_{\pm qn} = \langle \Psi^{(-)}_{1,2E} | \Psi(t) \rangle. \tag{4.11}$$

In the above expressions the following notations are used: the functions $\psi_n(x)$ and $\psi^{(-)}_{1,2E}$ are eigenstates of discrete and continuous spectra of the Hamiltonian (2.2) where $A \equiv 0$, with eigenenergies E_n and E. The subscripts 1 and 2 correspond to the positive and negative directions of the final momentum $\pm q$, $q = +\sqrt{2E}$, respectively. The wave function $\Psi(x,t)$ is the solution of the TDSE (2.1) at time $t > T$, where T is the moment when the pulse is switched off.

The spectral distribution $p_n(E)$ of electrons ejected with energy E, is given by a sum over directions of the final momenta,

$$p_n(E) = \frac{1}{2\pi}(|\mathcal{A}_{qn}|^2 + |\mathcal{A}_{-qn}|^2). \tag{4.12}$$

The factor $(2\pi)^{-1}$ fixes the normalization of the functions $\psi^{(-)}_{1,2E}(x)$.

Also, the probability $p_{n'n}$ of the transition to a bound final state $\Psi_{n'}$ is given by

$$p_{n'n} = |\langle \Psi_{n'} | \Psi(t) \rangle|^2. \tag{4.13}$$

By virtue of completeness of the basis set of functions $\psi^{(-)}_{1,2E}(x)$ and $\psi_n(x)$, the conservation law for the total probability has the form

$$\int_0^{+\infty} \frac{dE}{\sqrt{2E}} p_n(E) + \sum_{n'} p_{n'n} = 1. \tag{4.14}$$

The amplitudes $\mathcal{A}_{\pm qn}$ are a sum of three integrals for regions I, II, and W, correspondingly:

$$\mathcal{A}_{\pm qn} = \left(\int_{-\infty}^{a_-} + \int_{a_+}^{+\infty} + \int_{a_-}^{a_+} \right) \Psi^{(-)*}_{1,2E} \Psi\, dx. \tag{4.15}$$

If the solution of the problem (2.1) is known in the internal region W, e.g., as a result of some numerical calculations with the boundary conditions (4.3), then one can evaluate the integrals for regions I and II by continuing the internal solution into these regions with the help of the equations:

$$\Psi^{I,II}(x,t)=F_{as}^{I,II}(x,t)+\frac{i}{2}\{v_{as}^{I,II}(x,t)+w_{as}^{I,II}(x,t)\}, \tag{4.16}$$

and using the asymptotic form of functions $\psi_{1,2E}^{(-)}{}^{*}=\psi_{2,1E}^{(+)}$. These are listed in the table below:

	$\psi_{1E}^{(+)}$	$\psi_{2E}^{(+)}$
I	$e^{iqx}+\alpha e^{-iqx}$	βe^{-iqx}
II	βe^{iqx}	$e^{-iqx}+\gamma e^{iqx}$

where coefficients $\alpha(E)$, $\beta(E)$, and $\gamma(E)$ are the S-matrix elements for scattering on the potential V.

Let us introduce two integral transforms:

$$\hat{\Psi}^{I}(q,t)=\int_{-\infty}^{a_-}dx\, e^{iEt+iqx}\Psi(x,t) \tag{4.17}$$

and

$$\hat{\Psi}^{II}(q,t)=\int_{a_+}^{+\infty}dx\, e^{iEt-iqx}\Psi(x,t). \tag{4.18}$$

Making use of Eqs. (4.17), (4.18), and (4.15) one finds the following expression for the amplitudes:

$$\begin{pmatrix}\mathcal{A}_{-qn}\\ \mathcal{A}_{qn}\end{pmatrix}=\begin{pmatrix}\hat{\Psi}^{I}(q,t)\\ \hat{\Psi}^{II}(q,t)\end{pmatrix}+\begin{pmatrix}\alpha & \beta\\ \beta & \gamma\end{pmatrix}\begin{pmatrix}\hat{\Psi}^{I}(-q,t)\\ \hat{\Psi}^{II}(-q,t)\end{pmatrix}+\begin{pmatrix}\int_{a_-}^{a_+}\Psi_{2E}^{(-)}{}^{*}\Psi\,dx\\ \int_{a_-}^{a_+}\Psi_{1E}^{(-)}{}^{*}\Psi\,dx\end{pmatrix}, \tag{4.19}$$

where in the right-hand side, the time dependence at large t is only via a trivial phase factor.

Next, the solution $\Psi(x,t)$ extended into the external regions I and II with the help of Eq. (4.16), is substituted into Eqs. (4.17)–(4.18). Then the transforms $\hat{\Psi}^{I,II}(q,t)$ are expressed as a sum of the transformed parabolic potentials,

$$\hat{\Psi}^{I,II}(q,t)=\frac{i}{2}\hat{v}_{as}^{I,II}(q,t)+\frac{i}{2}\hat{w}_{as}^{I,II}(q,t), \tag{4.20}$$

where

$$\hat{v}^{I,II}(q,t)=\pm\int_{t_0}^{t}dt'\,\nu^{I,II}(t')\hat{G}_{as}^{I,II}(q,t;a_{\mp},t'), \tag{4.21}$$

and

$$\hat{w}^{I,II}(q,t)=\mp\int_{t_0}^{t}dt'\,\mu^{I,II}(t')D^{*\prime}\hat{G}_{as}^{I,II}(q,t;a_{\mp},t'). \tag{4.22}$$

In order to simplify calculations, we assume that all bound states including the initial state $\psi_n(x)$ are negligibly small in the regions I and II so that the terms $\hat{F}^{I,II}(q,t)$ can be discarded.

The mixed Green's functions $\hat{G}_{as}^{I,II}(q,t;x',t')$ above are obtained by applying transforms (4.17)–(4.18) to the Green's function $G_{as}(x,t;x',t')$, with respect to its first space variable x. The evaluation of the functions $\hat{G}_{as}^{I,II}$ gives

$$\hat{G}_{as}^{I,II}(q,t;x',t')=e^{\pm iq[\xi(t)+x'-\xi(t')]+iEt'}\Phi(z_{I,II}), \tag{4.23}$$

where

$$z_{I,II}=-q\sqrt{\frac{t-t'}{2}}\mp\frac{a_{\mp}-\xi(t)-x'+\xi(t')}{\sqrt{2(t-t')}}, \tag{4.24}$$

and $\Phi(z)$ is the Fresnel integral,

$$\Phi(z)=\frac{1}{\sqrt{\pi i}}\int_{z}^{+\infty}e^{i\rho^2}\,d\rho. \tag{4.25}$$

Thus, Eqs. (4.19)–(4.25) give the ionization amplitudes $\mathcal{A}_{\pm qn}$ in a closed form. These amplitudes are time independent for any $t>T$.

Now we consider the asymptotic representation of Eq. (4.19), generally, for large times $t\gg T$. In this case, the absolute values of the arguments z_I and z_{II} in the Fresnel integral (t' is fixed)

$$z_{I,II}=-q\sqrt{\frac{t}{2}}+O(t^{-1/2}),\quad t\to+\infty. \tag{4.26}$$

are large within the whole domain of the t' integration in Eqs. (4.21) and (4.22) except the vicinity of the upper limit t. On the other hand, one can expect that in the internal region W the wave function at large times contains mainly the bound states (if there are no zero modes in the potential V). This is because the scattered wave packet disperses over a large volume as t increases. Thus, the contribution to the integrals (4.21) and (4.22) from the vicinity of the upper limit t is small due to the small magnitude of μ and ν which are determined by the values of the bound states at the boundaries $a_{\pm}$. In the rest of the integration domain, the asymptotic expansion for the Fresnel integral $\Phi(z)$ [31] can be used:

$$\Phi(z)=\begin{cases}1+\dfrac{e^{i\pi/4}}{2z\sqrt{\pi}}e^{iz^2}+O(z^{-3}), & z\to-\infty,\\ \dfrac{e^{i\pi/4}}{2z\sqrt{\pi}}e^{iz^2}+O(z^{-3}), & z\to+\infty.\end{cases} \tag{4.27}$$

One can neglect the terms of order $1/z$ in the expansion (4.27), provided that the following condition is valid:

$$Et \gg 1. \tag{4.28}$$

In the latter case, no contribution from $\hat{\Psi}^{I,II}(-q,t)$ comes to the amplitude (4.19). Also, by virtue of orthogonality between the bound states ψ_n and the scattering states $\psi^{(-)}_{1,2E}$, the integrals over the internal region W in the expression (4.19) can be neglected. As a result, the transition amplitudes are determined in this approximation by $\Psi^{I,II}(q,t)$ only. Their final form in terms of the probability flux is given by

$$\mathcal{A}_{\pm qn} \simeq \pm e^{i\phi_\pm} \int_{t_0}^{t} dt'\, j[\Psi(x,t'), \Theta_{\pm q}(x,t')]|_{x=a_\pm}. \tag{4.29}$$

Here the values of the phases $\phi_\pm$ are not important for evaluation of the function $p_n(E)$ and the flux $j(t)$ is given by

$$j[\Psi,\Phi] = \frac{i}{2}\{\Psi D^*\Phi^* - \Phi^* D\Psi\}, \tag{4.30}$$

where $\Theta_k(x,t)$ is the Volkov function (3.23).

One can expect that expression (4.29) gives a reasonably accurate approximation for not very small energies E or for sufficiently large times t so that condition (4.28) is satisfied. The approximative equality in Eq. (4.29) becomes exact under simultaneous passing to the limits $t \to +\infty$ and $|a_\pm| \to +\infty$. Thus, in this limit, expression (4.29) represents the summing up of the probability flux through a remote surface over all times. The error in Eq. (4.29) is of order $(Et)^{-1/2}$ because it is determined by the leading neglected term $1/z$ in the asymptotic expansions (4.27). This quantity tells what part of the outgoing wave packet (its components with energy E) still remains in the domain W at the moment of time t.

Expression (4.29) can be also applied in the moving Kramers-Henneberger frame provided that the flux has been transformed correspondingly. In this case, the expression (4.29) is reduced to the time-energy Fourier transform of the wave function at the boundary which is fixed in the KH frame. Equation (3.10) in [12] corresponds to this method of evaluating the energy spectrum of photoelectrons.

V. NUMERICAL METHOD

Now we formulate a numerical method which will be applied below to solve a one-dimensional TDSE (2.1) on a time-space grid. In the velocity gauge, the 1D Hamiltonian $H(t)$ (2.2) takes the form:

$$H(t) = \frac{1}{2}p_x^2 - \frac{e}{c}A(t)p_x + V(x). \tag{5.1}$$

For time integration, we employ the Crank-Nicholson scheme that provides the accuracy of order $O(\tau^2)$ for each time step τ. The operator form of this scheme is

$$\left(I + \frac{i\tau}{2}H(t_{k+1/2})\right)\Psi^{k+1} = \left(I - \frac{i\tau}{2}H(t_{k+1/2})\right)\Psi^k,$$

$$t_k = t_0 + k\tau, \tag{5.2}$$

where the solution $\Psi^k(x)$ discretized with respect to time corresponds to $\Psi(x,t_k)$ and depends only on the space variable $x \in \mathbb{R}$. The time point $t_{k+1/2} = t_k + \tau/2$ is the intermediate point between t_k and t_{k+1}. This scheme will be implemented with the help of the Galerkin method (e.g., Ref. [32]). In this way, a system of algebraic finite difference equations is obtained at each step k. In the internal region W, the solution Ψ^k is sought as an expansion on a set of basis functions $\eta_j(x)$,

$$\Psi^k(x) = \sum_j u_j^k \eta_j(x), \quad x \in W. \tag{5.3}$$

Below in all calculations we use the cubic B splines [33] as a set of the basis functions $\eta_j(x)$.

Following the Galerkin method, one reduces Eq. (5.2) to the system of inhomogeneous algebraic equations with respect to $\mathbf{u}^{k+1}$, thus

$$\sum_j \left\{\hat{m}_{j'j} + \frac{i\tau}{2}\hat{h}^{k+1/2}_{0j'j}\right\}u_j^{k+1} - \sum_j \left\{\hat{m}_{j'j} - \frac{i\tau}{2}\hat{h}^{k+1/2}_{0j'j}\right\}u_j^k$$
$$= \frac{i\tau}{2}\eta_{j'}(a_+)\nu^{II}(t_{k+1/2}) - \frac{i\tau}{2}\eta_{j'}(a_-)\nu^{I}(t_{k+1/2}). \tag{5.4}$$

This system is a result of projecting Eq. (5.2) onto the functions $\eta_{j'}$. The matrix $\hat{m}$ is the overlap matrix, $\hat{m}_{j'j} = (\eta_{j'}, \eta_j)$. The Hermitian matrix $\hat{h}_0^{k+1/2}$

$$\hat{h}^{k+1/2}_{0j'j} = \int_{a_-}^{a_+} dx \left\{\frac{1}{2}\eta'_{j'}\eta'_j + \frac{ieA(t_{k+1/2})}{2c} \times (\eta_{j'}\eta'_j - \eta'_{j'}\eta_j) + V\eta_{j'}\eta_j\right\} \tag{5.5}$$

corresponds to the quadratic form for the second-order differential operator $H(t_{k+1/2})$ in Eq. (5.1) constructed on the elements η_j, without the surface terms. These latter are collected in the right-hand side of Eq. (5.4).

Thus, in order to close the system (5.4) (i.e., made it self-consistent) the boundary conditions are required to express $\nu^{I,II}(t_{k+1/2}) \approx (\nu^{I,II}_{k+1} + \nu^{I,II}_k)/2$ in terms of $\mu^{I,II}_k$ and $\mu^{I,II}_{k+1}$. To achieve this, let us consider the finite difference representation of Eq. (4.3) on the mesh grid t_k. The integrand contains the square root singularity at the end point t, so the quadrature rule chosen for the representation of the integral over time should take into account this singular point. The following rule on the uniform knot sequence with the step τ was chosen:

$$\int_0^{k\tau} t^{-1/2} f(t)\,dt \approx \sum_{s=0}^{k} a_s^{(k)} f(s\tau), \quad a_0^{(k)} = \frac{4\tau^{1/2}}{3},$$

$$a_k^{(k)} = a_0^{(k)}\{(k-1)^{3/2} - (k-3/2)k^{1/2}\}, \tag{5.6}$$

$$a_s^{(k)} = a_0^{(k)}\{(s-1)^{3/2} - 2s^{3/2} + (s+1)^{3/2}\}.$$

This composite rule is obtained by dividing the integration interval $[0,k\tau]$ into k subintervals $[s\tau, s\tau+\tau]$, $s = 0,1,\ldots,k-1$, and then applying to each subinterval the

simple weighted interpolatory rule [34] of the first degree of precision (i.e., exact on any polynomial of first degree) with the weight function $t^{-1/2}$.

With the help of rule (5.6), the finite difference representation of the boundary conditions takes the form

$$\nu_k^{I,II} = \pm \frac{(2\pi i)^{1/2}}{i a_0^{(k)}} \mu_k^{I,II} + f_k^{I,II}, \tag{5.7}$$

and $f_k^{I,II}$ is

$$f_k^{I,II} = -\sum_{s=0}^{k-1} \left(\frac{a_{k-s}^{(k)}}{a_0^{(k)}} \right) e^{iS_{ks}} \{ \nu_s^{I,II} - iP_{ks} \mu_s^{I,II} \} \mp \frac{(2\pi i)^{1/2}}{i a_0^{(k)}} 2F_{as}^{I,II}(t_k). \tag{5.8}$$

Here

$$S_{ks} = \frac{[\xi(t_k) - \xi(t_s)]^2}{2(t_k - t_s)}, \quad P_{ks} = \frac{\xi(t_k) - \xi(t_s)}{t_k - t_s} + \frac{e}{c} A(t_s). \tag{5.9}$$

Thus, using Eqs. (5.7), (5.3), and (5.4) one finds the final form of the system of algebraic equations,

$$\left(\hat{m} + \frac{i\tau}{2} \hat{h}^{k+1/2} \right) \mathbf{u}^{k+1} = \left(\hat{m} - \frac{i\tau}{2} \hat{h}^{k+1/2} \right) \mathbf{u}^k + \frac{i\tau}{2} \mathbf{d}^{k+1/2}, \tag{5.10}$$

where

$$\hat{h}_{j'j}^{k+1/2} = \hat{h}_{0j'j}^{k+1/2} + \frac{(2\pi i)^{1/2}}{2 i a_0^{(k)}} \{ \eta_{j'}(a_-) \eta_j(a_-) + \eta_{j'}(a_+) \eta_j(a_+) \}, \tag{5.11}$$

and

$$(\mathbf{d}^{k+1/2})_j = \eta_j(a_+) \frac{f_k^{II} + f_{k+1}^{II}}{2} - \eta_j(a_-) \frac{f_k^I + f_{k+1}^I}{2}. \tag{5.12}$$

The choice of functions η_j in the form of B splines generates the system (5.10) with band matrices. The inversion of such matrices can be efficiently carried out by the Gauss elimination method.

From the computational point of view, the main effort in solving Eq. (5.10) with a large number N_t of time steps comes from the need for summing up in the boundary equations (5.8). The computational time required for that grows as N_t^2, whereas the time required for inverting equations (5.10) grows as $N_x N_t$, where N_x is a number of the basis functions η_j (see also the discussion in Ref. [12]). For example, in our IBC calculations presented in the next section, we use $N_x = 200$ B splines. Then for $N_t = 10^4$, the evaluation of vectors $\mathbf{d}^k$ in Eq. (5.12) takes $\approx 80\%$ of the total computational time.

The time step τ for the integration of Eq. (5.1) with the laser pulse (6.5) was chosen to satisfy the condition $\tau U_p \ll 1$, where U_p is the ponderomotive potential. For $\omega = 0.1$ a.u., the step τ was typically taken to be 5×10^{-2} a.u. for $\mathcal{E}_0 = 0.1$ a.u., and 2.5×10^{-2} a.u. for $\mathcal{E}_0 = 0.2$ a.u.

VI. NUMERICAL RESULTS AND DISCUSSION

A. Model

For an illustration of the IBC method, we now consider the solution of the time-dependent Schrödinger equation that describes a one-dimensional atom modeled by the Pöschl-Teller potential $V_{PT}(x)$ [35]. This potential was used earlier in Ref. [12] and our results will allow a direct comparison to their work:

$$V_{PT}(x) = -\frac{V_0}{\cosh^2 x}, \quad |x| < \infty. \tag{6.1}$$

For $V_0 = 1$, this potential supports only one bound state,

$$\psi_0(x) = \frac{1}{\sqrt{2} \cosh x}, \tag{6.2}$$

with eigenenergy $E_0 = -0.5$ a.u., and a continuum of scattering states

$$\psi_{1,2E}^{(+)}(x) = \frac{iq \mp \tanh x}{1 + iq} e^{\pm iqx}. \tag{6.3}$$

It follows from Eq. (6.3) that there is an additional real pseudobound state, for $V_0 = 1$,

$$\psi_1(x) = \tanh x, \tag{6.4}$$

with $E = 0$. This state becomes a true bound state if the strength of the potential is increased by taking $V_0 > 1$.

The vector potential $A(t)$ generating the laser electric field $\mathcal{E}(t)$ was chosen in all calculations in the form of a square pulse,

$$A(t) = \begin{cases} -\dfrac{c\mathcal{E}_0}{\omega} \sin \omega t, & 0 \leqslant t \leqslant T = \dfrac{2\pi N}{\omega}. \\ 0, \quad t < 0, \quad t > T, \end{cases} \tag{6.5}$$

where the duration of the pulse T is defined in terms of N periods of the laser angular frequency ω.

B. Wave packets

First, we consider the integration of the TDSE, Eqs. (5.1), (6.1), and (6.5), with the atom being initially in the ground state (6.2). In these calculations, two sets of the peak field parameter $\mathcal{E}_0$ were used for an eight-cycle square pulse with $\omega = 0.1$ a.u.: (i) $\mathcal{E}_0 = 0.1$ a.u., and (ii) $\mathcal{E}_0 = 0.2$ a.u., with the excursion amplitude of the electron ξ_0 being 10 and 20 a.u., respectively.

Integration with respect to time was carried out for the full duration of the pulse, $0 \leqslant t \leqslant T$.

In all calculations by the IBC method the boundaries of the internal region W were taken to be $a_\pm = 10$ a.u. as shown in Fig. 1(a) and the integral boundary conditions (4.3) were imposed at $a_\pm$. The numerical solution in W was obtained

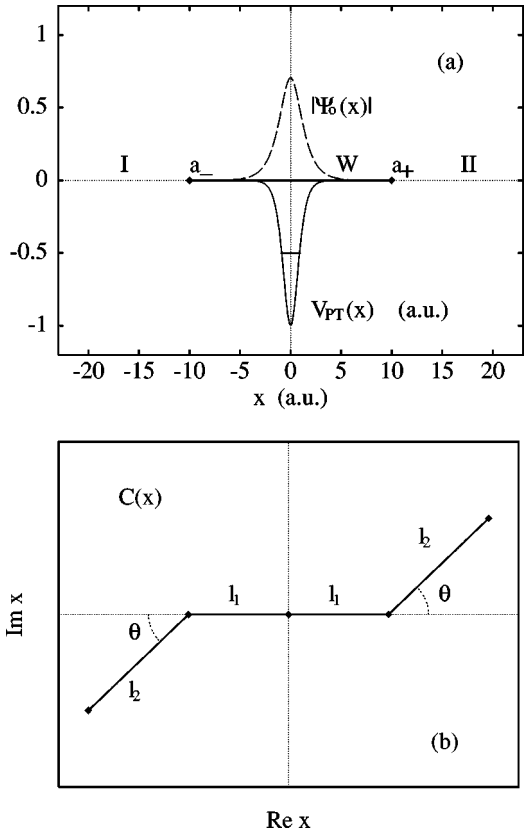

FIG. 1. (a) Division of space $\mathbb{R}$ into regions I, II, and W for integration by the IBC method. Boundaries of internal region W are $a_{\pm}=\pm 10$ a.u. The initial ground state (supported by the Pöschl-Teller potential) has eigenenergy $E_0=-0.5$ a.u. (b) The contour $C(x)$ in the complex x plane used in the CC calculations of the same problem.

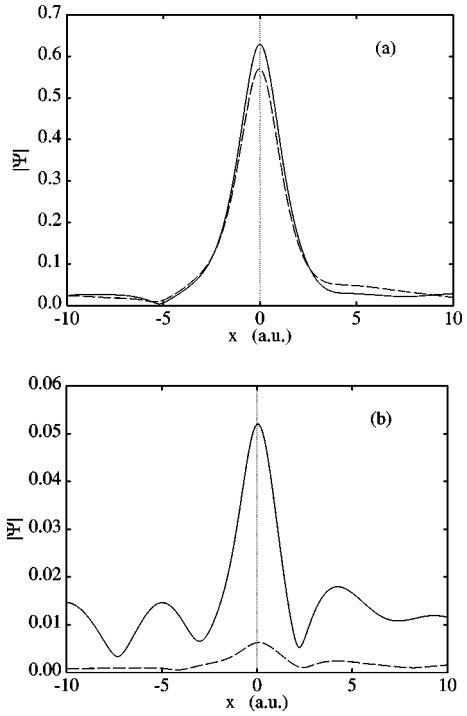

FIG. 2. Wave-packet dynamics after application of an eight-cycle square laser pulse with $\omega=0.1$ a.u. (a) $\mathcal{E}_0=0.1$ a.u.; (b) the same with $\mathcal{E}_0=0.2$ a.u. Solid curve—solution obtained by the IBC method; broken curve—solution obtained by the CC method. For the IBC method, boundaries are at ± 10 a.u. For the CC method, the contour $C(x)$ has parameters $l_1=l_2=10$ a.u. The best angle θ is 10° in (a) and 5° in (b).

by using the Crank-Nicholson-Galerkin method described above. Because the initial state (6.2) falls off exponentially, the terms $F_{as}^{I,II}$ in Eq. (4.3) at the boundaries are of order $\sim 10^{-5}$, and these terms were neglected. The potential V_{PT} vanishes even more rapidly, so that the solution could be accurately extended to the external regions I and II by using the asymptotic representation (4.16).

For comparison, the same problem has been also solved numerically (a) by the complex coordinate contour method [16] and (b) by imposing the rigid boundary conditions (2.3) at the outer edge of a very large space grid.

(a) CC method. The complex coordinate contour $C(x)$ is shown in Fig. 1(b) where l_1, l_2, and θ specify the integration domain on the complex plane x. The principal moment of this method is that the complex parts of $C(x)$ provide exponential decay of the functions $e^{ikC(x)}$ for $x>l_1$ and $e^{-ikC(x)}$ for $x<-l_1$. The rate of this decay depends on the angle θ, $0<\theta<\pi/2$.

Thus, the outgoing wave packets moving from the origin, disappear on the complex part of the contour $C(x)$ as they propagate past $\pm l_1$. Reflection of the wave packets from rigid boundaries that are taken sufficiently far from the origin is strongly suppressed in this case. The length l_2 and angle θ must be chosen in such a way that the outgoing wave packets are not appreciably scattered back towards the origin by the action of the electric field and potential beyond $\pm l_1$. At least two parameters, l_2 and θ, are needed to be specified while using the CC method. Below, for definiteness, we assume that $l_1=l_2$. Then only the angle θ is left to be adjusted to select a contour $C(x)$ best for integration. For too small angles θ, reflection takes place at the boundaries. On the other hand, if θ is too large this leads to a collapse of the scheme because the wave packets returning back to small x grow exponentially on the complex parts of the contour $C(x)$.

The wave packets obtained at the end of the pulse ($t=T$) by the CC method as well as by the IBC method, are displayed in Figs. 2(a) and 2(b). As shown in (b) below, the IBC results in these graphs are virtually exact.

In Fig. 2, we use a contour $C(x)$ with $l_1=l_2=10$ a.u. so that the length of the real part of $C(x)$ is taken the same as in the IBC calculations. The angle θ is chosen to achieve the best possible agreement with the IBC solution on the interval $-10\leqslant x\leqslant 10$. In Fig. 2(a), agreement between the CC and IBC is moderate. However, there is a huge difference between the wave packets in Fig. 2(b). This indicates that the chosen dimensions of $C(x)$ are too small. It follows, in fact, from our numerical experiments that for the field $\mathcal{E}_0=0.1$ a.u., l_1 should be taken at least 30 a.u., and for the field $\mathcal{E}_0=0.2$ a.u., at least 50 a.u. Thus, the size of the spatial grid which is required in the CC calculations is about ten times larger than the grid for the IBC method provided that we want to obtain a comparable accuracy of the numerical solutions.

(b) Rigid boundary method. As our numerical experiments show, the numerical solution which uses the reflective

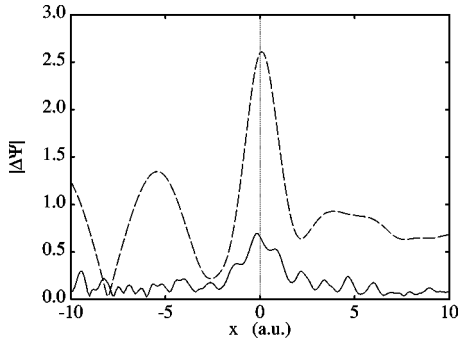

FIG. 3. Absolute difference $|\Delta\Psi|$ in units of 10^{-5}, between the solution obtained by the IBC method with $a_{\pm}=\pm 10$ a.u. and the rigid-boundary solution which uses a very large space grid ($a_{\pm} \approx \pm 1000$ a.u.): (i) solid curve—for $\mathcal{E}_0=0.1$ a.u., and (i) broken curve—for $\mathcal{E}_0=0.2$ a.u. Integration steps: $\Delta x=0.1$ a.u.; $\tau=5\times10^{-2}$ a.u. for (i) and $\tau=2.5\times10^{-2}$ a.u. for (ii).

(i.e., rigid boundary) conditions (2.3) needs spatial grids with the boundaries at least $a_{\pm}=\pm 1000$ a.u. for $\mathcal{E}_0=0.1$ a.u., and $a_{\pm}=\pm 1500$ a.u. for $\mathcal{E}_0=0.2$ a.u. These large grids are consistent with earlier calculations by Eberly and co-workers [36] who used the reflective boundary condition (2.3). In Fig. 3 we present the absolute difference between the solutions obtained by the IBC method and by the reflective boundary method (2.3), displayed in the interval $-10 \leqslant x \leqslant 10$ a.u. It can be seen that both solutions agree with each other to within 10^{-5}.

These results clearly demonstrate the superiority of the IBC method. We point out that the grid required in this method is determined by the decaying rate of the atomic potential $V(x)$ only. On the contrary, in the CC method as well as in the method which uses reflective conditions of type (2.3), the spatial grid size depends largely on the laser field parameters and has to be taken larger and larger as the quiver ξ_0 increases.

Finally, we note that similar difficulties exist in the method of Boucke *et al.* [12] where the Hamiltonian is assumed to be asymptotically field free. One needs to use the Kramers-Henneberger frame, and the size of the grid also depends on the quiver ξ_0. In the wave-packet calculations [12] which we have repeated here, Boucke *et al.* had to take the boundaries of the spatial grid at ± 50 a.u. (to compare with ± 10 a.u. in our calculations).

The IBC method allows also to take a scattering state (6.3) as the initial state for the TDSE. Then the solution gives cross sections for the free-free and free-bound laser-induced transitions. The excellent quality of the IBC continuum solutions can be ascertained by comparing with the exact calculations using large grids and proper logarithmic derivatives imposed at the boundaries. We note that the CC method cannot be applied in the latter case because the incident plane wave contained in the scattering state exponentially grows on the contour $C(x)$.

C. Energy distribution $p(E)$

First, we consider the energy spectrum of photoelectrons ejected by the laser pulse. The computed energy distribution $p(E)$ for the electrons which are initially in the ground state (6.2), is shown in Fig. 4 for several values of $\mathcal{E}_0$. The angular

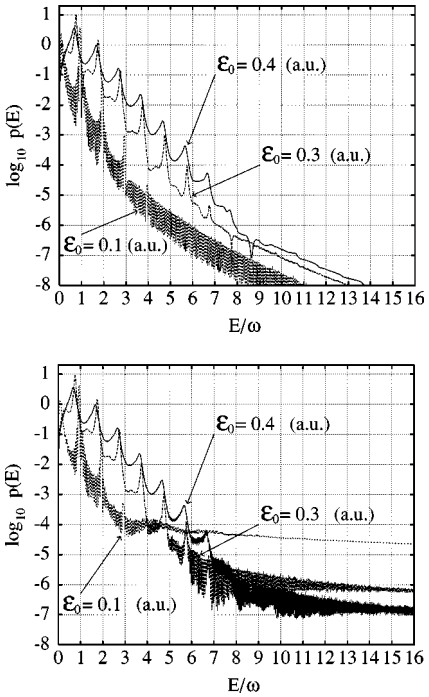

FIG. 4. The energy distribution $p(E)$ of laser-ejected electrons for several values of the field $\mathcal{E}_0$. A 16-cycle square laser pulse, with angular frequency $\omega=0.5$ a.u. The function $p(E)$ is obtained using (a) the full expression (4.19) for amplitudes, and (b) the asymptotic expression (4.29). The pondermotive shifts of the ATI peaks are clearly seen.

frequency ω of the field was chosen equal to the binding energy of the ground state $|E_0|$, $\omega=0.5$ a.u.

Taking into account the pondermotive shift U_p,

$$U_p=\frac{\mathcal{E}_0^2}{4\omega^2}, \tag{6.6}$$

the position E_n of the peaks in the spectra is approximately given by the equation

$$E_n=n\omega-|E_0|-U_p. \tag{6.7}$$

This corresponds to absorbing by the electron the energy of n photons. For the laser parameters used in Figs. 4, the pondermotive shifts U_p which enter Eq. (6.7), are 0.16, 0.09, and 0.01 a.u. for $\mathcal{E}_0=0.4$, 0.3, and 0.1 a.u., respectively. These values give a reasonable estimate of the exact numerical shifts obtained in the present calculations. A discussion of the peaks in the photoelectron spectra shown to be partly produced as a result of Stark-shifted bound-state multiphoton resonances can be found in Ref. [37].

The spectral distributions, shown in Figs. 4(a) and 4(b) have been obtained in two different ways. In Fig. 4(a), the spectral distributions $p(E)$ are calculated using the full amplitudes $\mathcal{A}_{\pm q0}$ (4.19)–(4.25). For $t=T$, this gives the exact result for $p(E)$. On the other hand, the distributions in Fig. 4(b) have been obtained using the flux expression (4.29), with t taken up to T. The latter is valid only under condition (4.28). It can be seen from Fig. 4 that for the particular choice of laser parameters, the asymptotic expression (4.29) gives a good estimate for the energy distribution $p(E)$. The

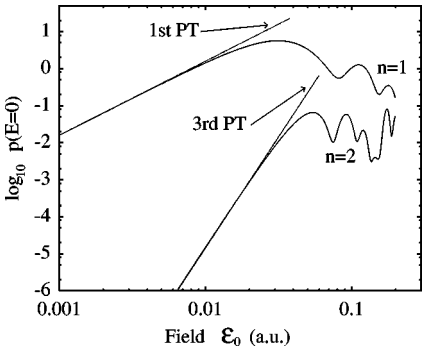

FIG. 5. Comparison between the exact calculations and perturbation theory. Probability density $p(E=0)$ as a function of the laser field $\mathcal{E}_0$, for the electron transition from the ground state with $E_0=-0.5$ a.u. to a pseudobound state with $E=0$. A 16-cycle laser pulse with angular frequency $\omega=0.5$ a.u. $(n=1)$ and eight-cycle pulse with $\omega=0.25$ a.u. $(n=2)$.

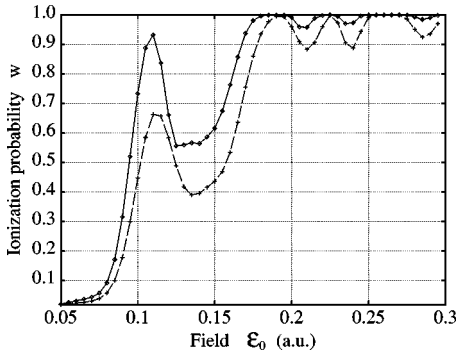

FIG. 6. Square laser pulse with angular frequency $\omega=0.2$ a.u. Variation of the ionization probability w with the laser field $\mathcal{E}_0$ at the end of a four-cycle (broken curve) and eight-cycle (solid curve) pulse.

positions and heights of the ATI peaks are correctly reproduced. However, at the bottom of continuum, the asymptotic expression (4.29) cannot be applied and one needs to use the full expression (4.19).

As Figs. 4 show, the asymptotic formula for $p(E)$ works better for stronger fields $\mathcal{E}_0$. Qualitatively, this is because the electrons leave domain W faster when exposed to stronger fields. For a fixed value of T, this facilitates the condition (4.28.) We also point out that the fast oscillations seen in some curves in Figs. 4 can be traced to the steep front of the pulse (6.5).

At small intensities of the field, the exact energy distributions $p(E)$ can be used for establishing the validity region of the standard perturbation theory.

As an illustration, we consider transitions from the (even-parity) ground state $\psi_0(x)$ of Eq. (6.2) to the (odd-parity) pseudobound state $\psi_1(x)$ of Eq. (6.4), with energy $E=0$.

As the first example, we take $\omega=|E_0|=0.5$ a.u. The leading term is one-photon absorption, $n=1$. In the lowest (first) order of perturbation theory, $p(E)$ is generally given by

$$p^{(1)}(E)=\frac{1}{2\pi}\sum_{s=1}^{2}\left|\int_0^T dt\, e^{i\Omega t}\langle\psi_{s,q}^{(-)}|\frac{e}{c}pA(t)|\psi_0\rangle\right|^2$$

$$=\frac{\pi\mathcal{E}_0^2\Omega}{\cosh^2\dfrac{\pi q}{2}}\,\frac{\sin^2\dfrac{(\Omega-\omega)}{2}T}{(\Omega^2-\omega^2)^2},\qquad \Omega=E-E_0. \tag{6.8}$$

A comparison between both methods for the transition to the $E=0$ level, is presented in Fig. 5 [''1st perturbation theory (PT)'' and ''$n=1$'' curves]. As can be seen, in this case, perturbation theory works well up to $\mathcal{E}_0\approx 0.01$ a.u.

As the second example, we take $\omega=0.25$ a.u. The leading term is now two-photon absorption. It follows immediately from the parity consideration that the second-order term $p^{(2)}(E=0)$ vanishes, and the leading term of perturbation theory is $p^{(3)}(E=0)$. In Fig. 5, the corresponding curves are marked ''3rd PT'' and ''$n=2$.'' The validity region of perturbation theory extends, in this case, up to $\mathcal{E}_0\approx 0.03$ a.u.

D. Ionization probability

For the comparison of our calculations with the calculations performed in Ref. [12], we evaluate the ionization probability of the atom, $w(\mathcal{E}_0)$,

$$w=1-p_{00} \tag{6.9}$$

where the ground-state probability p_{00} is given, at the end of the square pulse, by Eq. (4.13). As in Ref. [12], we used four- and eight-cycle pulses with the angular frequency $\omega=0.2$ a.u.

The curves (see Fig. 6) produced in these calculations are identical with the ionization curves in Fig. 3(a) of Ref. [12]. The ionization minima in Fig. 6 are due to the effect of channel closing caused by the dynamical shift of the free-electron energy, U_p, Eq. (6.6). Neglecting the ac Stark shift in the ground state, an n-photon channel is open only if

$$n\omega+E_0>U_p. \tag{6.10}$$

This formula gives at $\omega=0.2$ a.u. the threshold fields equal to $\mathcal{E}_0=0.13$, 0.22, and 0.28 a.u. for closing $n=3$, 4, and 5-photon channels. The second-order account of the ac Stark shift of the E_0 reduces these threshold values by some 6%. The minima positions in the calculated ionization probability are found to be in good agreement with the above estimate for $n=3$ and 5, but it is not as good for $n=4$ where $\mathcal{E}_0$ passes through the critical value 0.22 a.u. for the overbarrier ionization.

VII. CONCLUSIONS

We have applied the general theory of parabolic potentials to the solution of the time-dependent Schrödinger equation for an atom interacting with the classical laser field. The method is used to impose on the wave function the exact boundary conditions, on an intermediate surface in the configuration space. These conditions are then used in the numerical solution of the equation. In this way, the domain

where spatial integration must be carried out numerically can be substantially reduced. The method is based on dividing the configuration space into an internal domain where the quantum-mechanical description is required, and an external domain where the motion of the electron is assumed to be semiclassical. For short-range atomic potentials, the accurate asymptotic behavior of the solution is represented by the time-dependent Green's function for a free electron moving in the external (laser) electric field. This allows us to formulate integral boundary conditions on σ in terms of the asymptotic parabolic potentials. The long-range Coulomb potential can also be included into consideration. Numerical examples considered in the paper demonstrate the advantages of the present theory. The wave packets, energy spectra, and ionization probabilities have been obtained by this method and compared wherever possible with earlier calculations. Application of the method to 3D cases will be the subject of later publications.

[1] G. Floquet, Ann. Ec. Norm. **13**, 47 (1883); J. H. Shirley, Phys. Rev. **138B**, 979 (1965); S. I. Chu, Adv. At. Mol. Phys. **21**, 197 (1985).

[2] M. Pont, D. Proulx, and R. Shakeshaft, Phys. Rev. A **44**, 4486 (1991); R. M. Potvliege and R. Shakeshaft, Adv. At., Mol., Opt. Phys. **1**, 373 (1992); B. Piraux and R. Shakeshaft, Phys. Rev. A **49**, 3903 (1994).

[3] P. G. Burke, P. Franken, and C. J. Joachain, J. Phys. B **24**, 761 (1991); O. Latinne, N. J. Kylstra, M. Dörr, J. Purvis, M. Terao-Dunseath, C. J. Joachain, P. G. Burke, and C. J. Noble, Phys. Rev. Lett. **74**, 46 (1995).

[4] J. H. Eberly, R. Grobe, C. K. Law, and Q. Su, Adv. At., Mol., Opt. Phys. **1**, 301 (1992).

[5] K. C. Kulander, Phys. Rev. A **35**, 445 (1987); K. C. Kulander, K. J. Schafer, and J. L. Krause, Phys. Rev. Lett. **66**, 2601 (1991); K. C. Kulander, K. J. Schafer, and J. L. Krause, Adv. At., Mol., Opt. Phys., Suppl. **1**, 247 (1992); O. Latinne, C. J. Joachain, and M. Dörr, Europhys. Lett. **26**, 333 (1994).

[6] K. C. Kulander, Phys. Rev. A **36**, 2726 (1987); a Hartree-Fock model for the helium atom and two-electron treatment of the same problem is by J. S. Parker, K. T. Taylor, C. W. Clark, and S. Blodgett-Ford, J. Phys. B **29**, L33 (1996); A. Scrinzi and B. Piraux, Phys. Rev. A **58**, 1310 (1998); D. Dundas, K. T. Taylor, J. S. Parker, and E. S. Smyth, J. Phys. B **32**, L231 (1999) using different methods of an explicit account of the electron-electron interaction in the Schrödinger equation.

[7] S. Chelkowski, C. Foisy, and A. D. Bandrauk, Phys. Rev. A **57**, 1176 (1998).

[8] H. Yu and A. D. Bandrauk, Phys. Rev. A **56**, 685 (1997); A. D. Bandrauk and H. Yu, *ibid.* **59**, 539 (1999).

[9] M. Gavrila, Adv. At., Mol., Opt. Phys., Suppl. **1**, 435 (1992).

[10] J. C. Wells, I. Simbotin, and M. Gavrila, Phys. Rev. A **56**, 3961 (1997).

[11] D. R. Schultz, M. R. Strayer, and J. C. Wells, Phys. Rev. Lett. **82**, 3976 (1999).

[12] K. Boucke, H. Schmitz, and H.-J. Kull, Phys. Rev. A **56**, 763 (1997).

[13] A. Goldberg and B. W. Shore, J. Phys. B **11**, 3339 (1978); C. Leforestier and R. E. Wyatt, J. Chem. Phys. **78**, 2334 (1983); R. Kosloff and D. Kosloff, J. Comput. Phys. **63**, 363 (1986); D. Neuhauser and M. Baer, J. Chem. Phys. **90**, 4351 (1989); U. V. Riss and H.-D. Meyer, J. Phys. B **28**, 1475 (1995); **31**, 2279 (1998).

[14] J. L. Krause, K. J. Schafer, and K. C. Kulander, Phys. Rev. A **45**, 4998 (1992).

[15] R. Heather and H. Metiu, J. Chem. Phys. **86**, 5009 (1987); T. Millack, Phys. Rev. A **48**, 786 (1993); A. Keller, *ibid.* **52**, 1450 (1995).

[16] C. W. McCurdy and C. K. Stroud, Comput. Phys. Commun. **63**, 323 (1991); T. N. Rescigno, M. Baertschy, D. Byrum, and C. W. McCurdy, Phys. Rev. A **55**, 4253 (1997).

[17] A general discussion of the size of the configuration space required for studying various laser-induced processes can be found in K. C. Kulander, K. J. Schafer, and J. L. Krause, Adv. At., Mol., Opt. Phys., Suppl. **1**, 247 (1992). See also K. Kulander, Phys. Rev. A **35**, 445 (1987) for MPI; K. J. Schafer and K. C. Kulander, *ibid.* **42**, 5794 (1990) for ATI; and J. L. Krause, K. J. Schafer, and K. C. Kulander, *ibid.* **45**, 4998 (1992) for HHG (in hydrogen).

[18] P. G. Burke and K. A. Berrington, *Atomic and Molecular Processes: An R-matrix approach* (IOP Publications, Bristol, 1993).

[19] H. W. Jang and J. C. Light, J. Chem. Phys. **99** (2), 1057 (1993).

[20] P. G. Burke and V. Burke, J. Phys. B **30**, L383 (1997).

[21] H. A. Kramers, in *Collected Scientific Papers* (North-Holland, Amsterdam, 1956); W. C. Henneberger, Phys. Rev. Lett. **31**, 838 (1968); H. L. Cycon, R. G. Froese, W. Kirsch, and B. Simon, in *Schrödinger Operators with Applications to Quantum Mechanics and Global Geometry* (Springer-Verlag, New York, 1987), Chap. 7.

[22] S. G. Mikhlin, *Linear Equations of Mathematical Physics* (Holt, Rinehardt and Winston, New York, 1967), and references therein.

[23] M. C. Gutzwiller, *Chaos in Classical and Quantum Mechanics* (Springer-Verlag, New York, 1991), Chap. 12.

[24] V. P. Maslov and M. V. Fedoriuk, *Semiclassical Approximation in Quantum Mechanics* (Reidel, Boston, 1981).

[25] Reference [22], particularly, Chap. 6 by P. M. Riz and L. N. Slobodetsky.

[26] A similar situation takes place, for instance, in the heat flow problems, see e.g., L. D. Landau and E. M. Lifshitz, *Fluid Mechanics* (Pergamon Press, New York, 1995), p. 203 where integral-boundary conditions may occur in the form of a constraint between the temperature and the heat flux. This example has been earlier pointed out in Ref. [12].

[27] As was, probably, first pointed out by Feynman, the construction of an exact Green's function for a particle moving semiclassically is possible if the potential is linear or quadratic in coordinates (which is our case). The potential can then be an arbitrary function of time. See R. P. Feynman, Rev. Mod. Phys. **20**, 367 (1948); also R. P. Feynman and A. R. Hibbs, *Quantum Mechanics and Path Integrals* (McGraw-Hill, New York, 1965).

[28] R. G. Newton, *Scattering Theory of Waves and Particles* (Springer-Verlag, New York, 1982), Chap. 18; S. P. Merkuriev

and L. D. Faddeev, *Quantum Scattering Theory for Few-Body Systems* (Nauka, Moscow, 1985), in particular, Chap. V.

[29] L. D. Landau and E. M. Lifshitz, *Quantum Mechanics (Non-relativistic Theory)* (Pergamon Press, Oxford, 1975), Chap. VII.

[30] A. M. Perelomov, V. S. Popov, and M. V. Terentiev, Zh. Éksp. Teor. Fiz. **50**, 1383 (1966) [Sov. Phys. JETP **23**, 424 (1966)]; S. Geltman, J. Phys. B **10**, 831 (1977).

[31] M. Abramowitz and I. Stegun, *Handbook of Mathematical Functions*, 10th ed., Natl. Bur. Stand. (U.S.) Appl. Math. Ser. No. 55 (U.S. GPO, Washington, DC, 1972), p. 295.

[32] V. A. Trenogin, *Functional Analysis* (Nauka, Moscow, 1980), p. 331; E. B. Becker, G. F. Carey, and J. T. Oden, *Finite Elements, An Introduction* (Prentice-Hall, Englewood Cliffs, NJ, 1981), Vol. I.

[33] C. de Boor, *A Practical Guide to Splines* (Springer-Verlag, New York, 1978), p. 108.

[34] E. Isaacson and H. B. Keller, *Analysis of Numerical Methods* (Jonh Wiley & Sons, New York, 1966) p. 331.

[35] G. Pöschl and E. Teller, Z. Phys. **83**, 143 (1933).

[36] J. Javanainen, J. H. Eberly, and Q. Su, Phys. Rev. A **38**, 3430 (1988).

[37] V. C. Reed and K. Burnett, Phys. Rev. A **43**, 6217 (1991).